Cardiovascular Drugs and Therapy (2022) 36:1047–1059
https://doi.org/10.1007/s10557-021-07227-6

ORIGINAL ARTICLE

Flavocoxid Ameliorates Aortic Calcification Induced by Hypervitaminosis D_3 and Nicotine in Rats Via Targeting TNF-α, IL-1β, iNOS, and Osteogenic Runx2

Ahmed E. Amer[1,2] · George S. G. Shehatou[1,2] · Hassan A. El-Kashef[1,2] · Manar A. Nader[2] · Ahmed R. El-Sheakh[2]

Accepted: 6 July 2021 / Published online: 26 July 2021

Abstract

Purpose This research was designed to investigate the effects and mechanisms of flavocoxid (FCX) on vascular calcification (VC) in rats.

Methods Vitamin D_3 and nicotine were administered to Wistar rats, which then received FCX (**VC-FCX group**) or its vehicle (**VC group**) for 4 weeks. Control and FCX groups served as controls. Systolic (SBP) and diastolic (DBP) blood pressures, heart rate (HR), and left ventricular weight (LVW)/BW were measured. Serum concentrations of calcium, phosphate, creatinine, uric acid, and alkaline phosphatase were determined. Moreover, aortic calcium content and aortic expression of runt-related transcription factor (Runx2), osteopontin (OPN), Il-1β, α-smooth muscle actin (α-SMA), matrix metalloproteinase-9 (MMP-9), inducible nitric oxide synthase (iNOS), and tumor necrosis factor-α (TNF-α) were assessed. Oxidative status in aortic homogenates was investigated.

Results Compared to untreated VC rats, FCX treatment prevented body weight loss, reduced aortic calcium deposition, restored normal values of SBP, DBP, and HR, and attenuated LV hypertrophy. FCX also improved renal function and ameliorated serum levels of phosphorus, calcium, and ALP in rats with VC. FCX abolished aortic lipid peroxidation in VC rats. Moreover, VC-FCX rats showed marked reductions in aortic levels of Il-1β and osteogenic marker (Runx2) and attenuated aortic expression of TNF-α, iNOS, and MMP-9 proteins compared to untreated VC rats. The expression of the smooth muscle lineage marker α-SMA was greatly enhanced in aortas from VC rats upon FCX treatment.

Conclusion These findings demonstrate FCX ability to attenuate VDN-induced aortic calcinosis in rats, suggesting its potential for preventing arteiocalcinosis in diabetic patients and those with chronic kidney disease.

Keywords Vascular calcification · Flavocoxid · Vitamin D_3 · Nicotine · Runx2 · TNF-α

Introduction

Vascular calcification (VC) is a pathogenic status of vessel wall mineralization. Aging and many disease conditions, including diabetes mellitus, atherosclerosis, and chronic kidney disease (CKD), are associated with VC [1].

VC may take place in either the intimal or medial layers of the arterial wall. Intimal calcification occurs as discrete or diffuse deposits in the intima and is associated with focal atherosclerotic plaques. It might be a result of an inflammatory response to subintimal lipid deposition, macrophage accumulation, and atherogenic plaque formation. Medial calcification occurs in the absence of atheroma and is linked to advanced age, hypertension, diabetes mellitus, and CKD. It occurs as linear sheets of hydroxyapatite calcium crystals in the center of the medial layer, leading to vascular stiffening [2–4].

During VC, vascular smooth muscle cells (VSMCs) experience a phenotypic transition from a contractile to an osteogenic phenotype [5–7]. This phenotype shift is accompanied by a downregulated expression of smooth muscle lineage

✉ George S. G. Shehatou
georgeshehatou@gmail.com; gsgskh@mans.edu.eg

[1] Department of Pharmacology and Biochemistry, Faculty of Pharmacy, Delta University for Science and Technology, International Coastal Road, Gamasa City, Dakahliya, Egypt

[2] Department of Pharmacology and Toxicology, Faculty of Pharmacy, Mansoura University, Mansoura, Dakahliya, Egypt

markers such as α-smooth muscle actin (α-SMA) and enhanced expression of osteogenic markers such as alkaline phosphatase (ALP), osteocalcin, osteopontin (OPN), and runt-related transcription factor (Runx2) [6, 7].

Multiple mechanisms are involved in medial vascular calcinosis, including induction of a systemic inflammatory state and elevations in vascular oxidative stress [8, 9]. Vitamin D3 plus nicotine (VDN)-induced medial calcification in rats was associated with increased mRNA expression of tumor necrosis factor-alpha (TNF-α) and interleukin-1 beta (IL-1β) [10]. Inflammatory cytokines, oxidative stress, and hyperphosphatemia are among the main pathological insults that elicit transdifferentiation of VSMCs into osteoblast-like cells [11–13]. Moreover, enhanced vascular generation of reactive oxygen species (ROS) can enhance the overexpression of pro-inflammatory genes that may contribute to the development and progression of VC [14].

Additionally, inflammatory cytokines can increase the expression of inducible nitric oxide synthase (iNOS) and matrix metalloproteinase (MMP)-1,3 and 9 [15]. iNOS expression may enhance VC by affecting alkaline phosphatase (ALP) activity [16]. MMPs degrade elastin, the main constituent of elastic fibers, initiating medial calcification [17, 18].

The VDN rat model, initially developed by Niederhoffer et al. [19], is an established model of VC, which mimics the pathogenesis of vessel calcification in aging, diabetes, and end-stage renal disease [20]. Hypervitaminosis D3 elicits excessive calcium deposition in vessel walls [21]. Nicotine enhances the release of catecholamines and increases calcium burden in blood vessels [22].

Flavocoxid (FCX), a proprietary mixture of two flavonoids; baicalin and catechin, exhibits inhibitory activity of both cyclooxygenase and 5-lipoxygenase [23, 24]. FCX offered strong antioxidant potential and diminished production of inflammatory cytokines and iNOS in cell assays and in vivo experimental models [24–32].

Additionally, FCX ameliorated high cholesterol diet (HCD)-induced vascular dysfunction in rabbits via its antioxidant and anti-inflammatory properties [33]. Many studies showed that the flavonoid constituents of FCX have beneficial effects on the vascular system. Baicalin reduced blood pressure and attenuated aortic contractile responses to vasoconstrictors via modulating intracellular Ca^{2+} regulation in spontaneously hypertensive rats [34]. Baicalin also diminished vascular inflammation and oxidative stress induced by high glucose treatment of cultured endothelial cells [35]. Catechin normalized blood pressure and attenuated endothelial dysfunction in prediabetic rats [36]. Moreover, catechin metabolite reduced monocyte adhesion to IL-1β–stimulated endothelial cells [37].

Since it was shown that FCX exerted greater effects than its individual flavonoids [28], it was of great interest to investigate the effects and mechanisms of FCX treatment on VDN-induced VC in rats.

Materials and Methods

Materials

FCX (Limbrel, 250 g/capsule) was bought from Pimus Pharmaceutical Inc. (Scottsdale, AZ, USA), vitamin D_3 (Devarol-S ampoules) was purchased from Memphis Company for Pharmaceutical & Chemical Industry (Cairo, Egypt). Nicotine was obtained from Merck KGaA company (Darmstadt, Germany).

Animals

Thirty-two male 8-week-old Wistar rats (180–220 g) were bought from the Holding Company for Biological Products and Vaccines (VACSERA, Giza, Egypt) and were left for acclimatization for one week before use. Rats were kept at room temperature with a 12 h on/off light cycle. The animal management guidelines of the Committee of Ethics of Scientific Research, Faculty of Pharmacy, Mansoura University, Egypt were applied during the handling of animals and experimentation.

Vascular Calcification Model and Animal Grouping

Rats were randomly assigned into four groups ($n = 8$/group), namely **control**, **FCX**, **VC,** and **VC-FCX** groups. **Control group** received normal saline (2.5 ml/kg/day, orally) for 30 days. **FCX group** received FCX (20 mg/kg /day, dissolved in normal saline, orally) for 30 days. **VC group** received VDN on day 1 of the experiment [vitamin D_3 (Devarol-S ampoules; a single dose of 300.000 IU/Kg, IM) and nicotine (two doses of 25 mg/kg, at 9 am and 6 pm, orally)], as previously described [10, 19, 38, 39]. **VC-FCX** group received FCX (20 mg/kg /day, orally) from the second day following VDN administration and continued and for 4 weeks. The chosen dose of FCX is equivalent to the human dose of 250 mg/day [40, 41]. This dose was previously reported to be effective in other inflammatory conditions in rats [27, 29, 42].

Experimental Assessments

At the end of the experiment (day 31), rats were weighed, and systolic (SBP) and diastolic (DBP) blood pressures were measured from conscious rats by a noninvasive tail-cuff system (ML125 NIBP, ADinstruments, Australia). Rats were then anesthetized with secobarbital (50 mg/kg) and an electrocardiogram (ECG) was acquired using a single channel device (Fakuda ME Kogyo Co. Ltd., Model:501-B III, Tokyo, Japan). The heart rate (HR) was calculated from the ECG charts.

Immediately afterward, rats were humanely killed. Blood was collected from the retro-orbital plexus, allowed to stand

for 30 min, and then centrifuged (1000 g, 15 min) to separate serum, for determination of levels of creatinine (CRCO-0600), uric acid (AUML-0427), calcium (CALA-0600), phosphorus (PHOS-0600), and ALP activity (PASL-0230) using commercial kits (ELITech Clinical Systems, France).

Moreover, the heart was removed and weighed to determine the heart weight/body weight (HW/BW) ratio. The left ventricle (LV) was dissected free from the heart tissues for calculation of LV weight (LVW)/BW and LVW/HW ratios.

Furthermore, the thoracic aorta was isolated and sectioned into ~1–1.5 cm segments for histological and immunohistochemical studies, homogenate preparation (5% (*w*/*v*) in phosphate-buffered saline (PBS)), and determination of calcium content.

Aortic tissue homogenates were used for measurement of malondialdehyde (MDA), reduced glutathione (GSH), and superoxide dismutase (SOD) activity using kits (MD2529, GR2511, and SD2521, respectively, Biodiagnostic, Cairo, Egypt). ELISA kits were used to determine aortic levels of IL-1β (E0119Ra, Bioassay Technology Laboratory, China), Runx2, and OPN (CSB-EL020594RA and CSB-E08393r, respectively, Cusabio, China).

Calcium Content of Aorta

Sections of the aorta (~100 mg of descending abdominal aorta) [43] were decalcified for 24 h with 0.6 N HCl. The calcium content of the HCl supernatant was calorimetrically determined by the o-cresolphthalein complexone method (Wei et al., 2013) using a kit (1001062) provided by Spinreact (Spain).

Histology and Immunohistochemical Staining

Portions of the left ventricle and aorta were fixed in 10% buffered formalin solution, embedded in paraffin, sliced, and dewaxed. The heart tissues were stained with hematoxylin and eosin (H&E), while aortic sections were stained by von Kossa stain for visualization of calcium as black deposits, as described previously [44]. ImageJ software (National Institutes of Health, USA) was used to analyze acquired aortic images for the determination of percentage area of black staining (calcium deposition). Microimages were imported to ImageJ software and 4–5 fields from each rat aorta were analyzed to calculate the average percentage of calcified area for each rat [45].

Immunohistochemical staining was applied to aortic sections using UltraVision detection system provided by Thermo Fisher Scientific, UK. Anti-α-SMA (AM128-5 M) and Anti-MMP-9 (AN816-5 M) were purchased from Biogenx (BioGenex Laboratories, San Ramon, CA, USA). Anti-TNF-α (RA0316-C.5) was from Scytek Laboratories (Logan, UT, USA) and Anti-iNOS (A14031) was purchased from ABclonal (Woburn, MA, USA). Immunostaining was quantified as the number of immunopositive cells for stained proteins per high power field (HPF) using ImageJ Software, as previously reported [46–48].

Statistical Analyses

Data are presented as means ± standard error of the mean (SEM). GraphPad Prism software (San Diego, CA, USA) was used to calculate the statistical significance of the results (two-way analysis of variance (ANOVA) followed by Tukey's post hoc test). The threshold of statistical significance was set at $p < 0.05$.

Results

General Characteristics and Physiologic Measures of Rats (Table 1)

VC rats showed a significant reduction in BW compared to the control group ($p < 0.0001$). FCX treatment prevented BW loss in VC rats. However, they still gained less weight than control rats ($p < 0.0001$ relative to both control and VC groups).

Moreover, FCX treatment improved hemodynamic and cardiac function in VC rats. FCX administration to VC rats abolished rises in SBP and DBP, restoring their values to those of controls ($p > 0.05$ vs. control group).

Furthermore, significant increases in HW/BW (by 28.6%, $p < 0.05$) and LVW/BW (by 95.1%, $p < 0.001$) indices were observed in the VC group relative to control rats. FCX elicited a marked decrease in LVW/BW (by 30.5%, $p < 0.05$), compared to the untreated VC group. These data are shown in Table 1.

ECG signals recorded from VC rats showed marked bradycardia, while VC-FCX rats showed insignificantly different heart rhythm compared to the control group **(**Fig. 1a**).** Microscopic pictures of H&E-stained heart tissues showed normal histology of cardiac muscles in control and FCX groups (Fig. 1b). Left ventricular tissues from the VC group exhibited hypertrophy and disarray of the cardiac myofibers. Heart sections from VC-FCX rats demonstrated reduced hypertrophy of cardiac myofibers.

Serum Biochemical Parameters (Table 2)

VC rats exhibited significant increases in serum levels of creatinine (by 267.2%), uric acid (by 241.8%), phosphorus (by 21.2%), and ALP (by 694.7%) when compared to control values ($p < 0.0001$ for all). Moreover, a significant decrease in serum calcium levels in the VC group was observed compared with levels in control rats (by 26.4%, $p < 0.0001$).

Table 1 General characteristics of rats at the end of the experiment

	Control	FCX	VC	VC-FCX
BW change (g)	69.50 ± 3.73	72.88 ± 3.65	−20.25 ± 2.78*	25.75±2.99*#
SBP (mmHg)	84.33 ± 4.68	85.83 ± 3.03	104.80 ± 2.52*	87.33±2.01#
DBP (mmHg)	64.17 ± 4.01	63.33 ± 2.42	86.83 ± 6.83*	66.33±2.01#
HR (Beats/min)	401.00 ± 7.09	389.5 ± 12.03	284.70 ± 20.75*	401.50±10.02#
HW/BW (mg/g)	2.95 ± 0.05	2.86 ± 0.05	3.79 ± 0.32*	3.31±0.15
LVW/BW (mg/g)	0.63 ± 0.07	0.69 ± 0.04	1.23 ± 0.14*	0.85±0.03#

Data are shown as means ± SEM, $n = 6–8$ rats per group

*, # $p < 0.05$ vs. control and VC groups, respectively

BW, body weight; DBP diastolic blood pressure; FCX, flavocoxid; HR, heart rate; HW, heart weight; LVW, left ventricular weight; SBP, systolic blood pressure; VC, vascular calcification

FCX ameliorated renal function in VC rats, where it returned serum concentrations of creatinine and urea to values that are insignificantly different from those of control rats. Moreover, treatment of VC rats with FCX restored serum phosphorus levels to near-normal values. Furthermore, VC-FCX rats exhibited significantly lower serum ALP levels (by

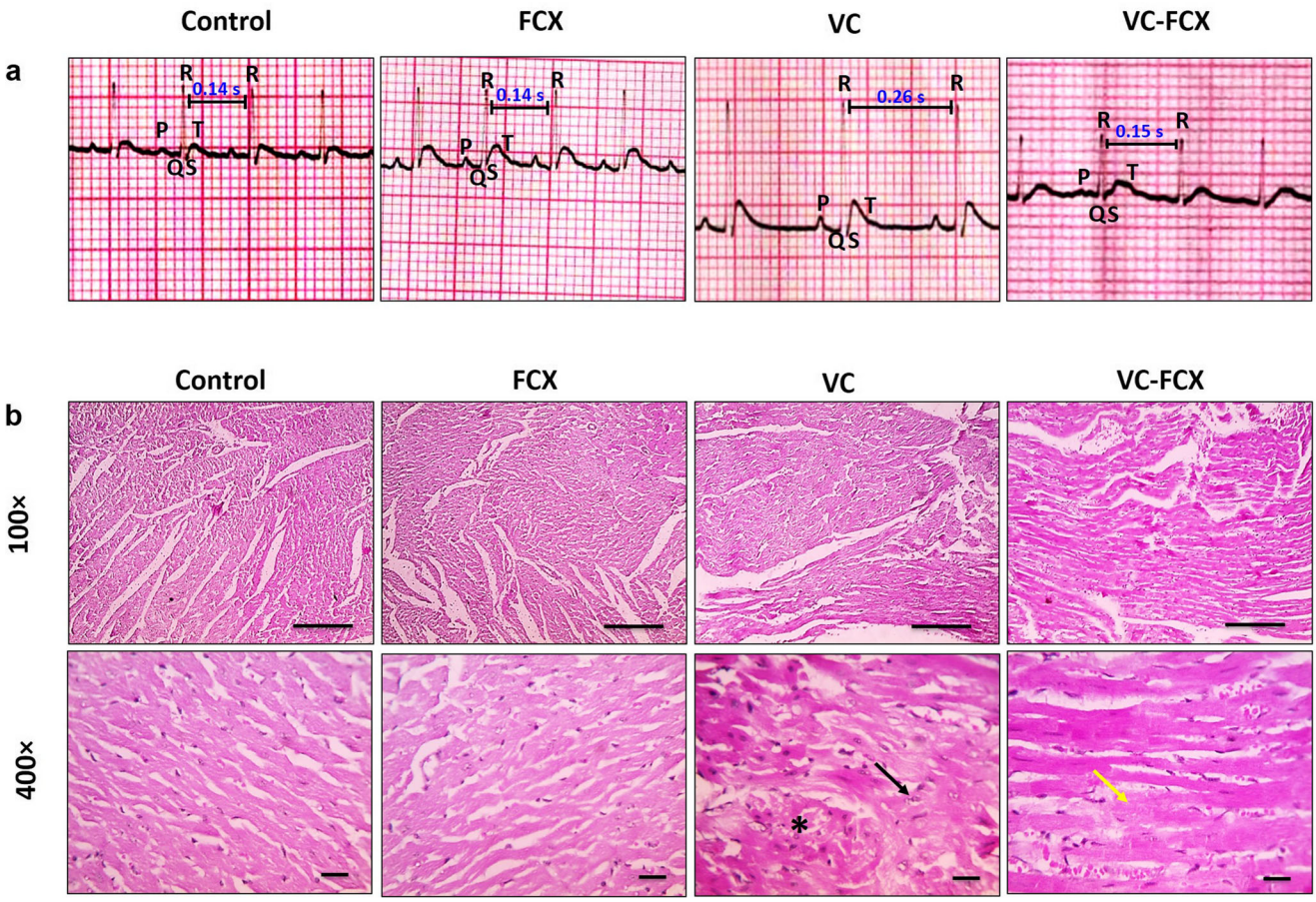

Fig. 1 Flavocoxid ameliorated VC-associated cardiac changes in hypervitaminosis D_3 plus nicotine-administered rats. **(a)** Representative ECG recordings for all groups. Heart rates were calculated from ECG traces according to the following formula [49]: Heart rate = 60/RR interval (seconds), where RR interval is the time between two successive R wave peaks. An increased RR interval was observed in the ECGs from VC rats relative to those of control, FCX, and VC-FCX groups, indicating a marked slowing of heart rate compared with those of the control group. FCX administration to the VC group resulted in the restoration of normal heart rhythm. **(b)** Representative microscopic pictures of H&E-stained rat hearts. The black arrow denotes ventricular hypertrophy and the * sign marks disarray of the cardiac myofibers. The yellow arrow shows decreased hypertrophy of cardiac myofibers in the VC-FCX group. ECG, electrocardiogram; FCX, flavocoxid; H&E, hematoxylin and eosin; VC, vascular calcification

Table 2 Flavocoxid improved renal function and ameliorated serum levels of phosphorus, calcium, and ALP in hypervitaminosis D_3 plus nicotine-administered rats

	Control	FCX	VC	VC-FCX
Serum creatinine (mg/dL)	0.64 ± 0.04	0.71 ± 0.03	2.35 ± 0.13*	0.57±0.02#
Serum uric acid (mg/dL)	0.98 ± 0.07	0.94 ± 0.05	3.35 ± 0.15*	1.14±0.05#
Serum phosphorus (mg/dL)	6.83 ± 0.17	6.60 ± 0.22	8.28 ± 0.17*	7.10±0.04#
Serum calcium (mg/dL)	11.00 ± 0.17	10.88 ± 0.24	8.10 ± 0.18*	9.80±0.34*#
Serum ALP (U/L)	56.25 ± 5.62	61.13 ± 4.49	447.00 ± 37.28*	183.60±11.64*#

Data are shown as means ± SEM, $n = 8$ rats per group

*, # $p < 0.05$ vs. control and VC groups, respectively

ALP, alkaline phosphatase; FCX, flavocoxid; VC, vascular calcification

58.9%, $p < 0.0001$) and significantly higher serum calcium levels (by 21.0%, $p < 0.001$) compared to the untreated VC group. These data are presented in Table 2.

Aortic Calcification

von Kossa staining of aortic tissues is shown in Fig. 2a. Calcified black areas in acquired microimages were quantified (Fig. 2b). The walls of the aortas from the control group did not show any calcium deposits. On the other hand, aortas from the VC group displayed extensive black staining of calcium deposition (percentage calcified area = 59.4 ± 6.3%, $p < 0.0001$ relative to control). Aortas from VC-FCX rats showed reduced calcium deposition, which was displayed as rows of black stained calcium particles parallel to tunica media

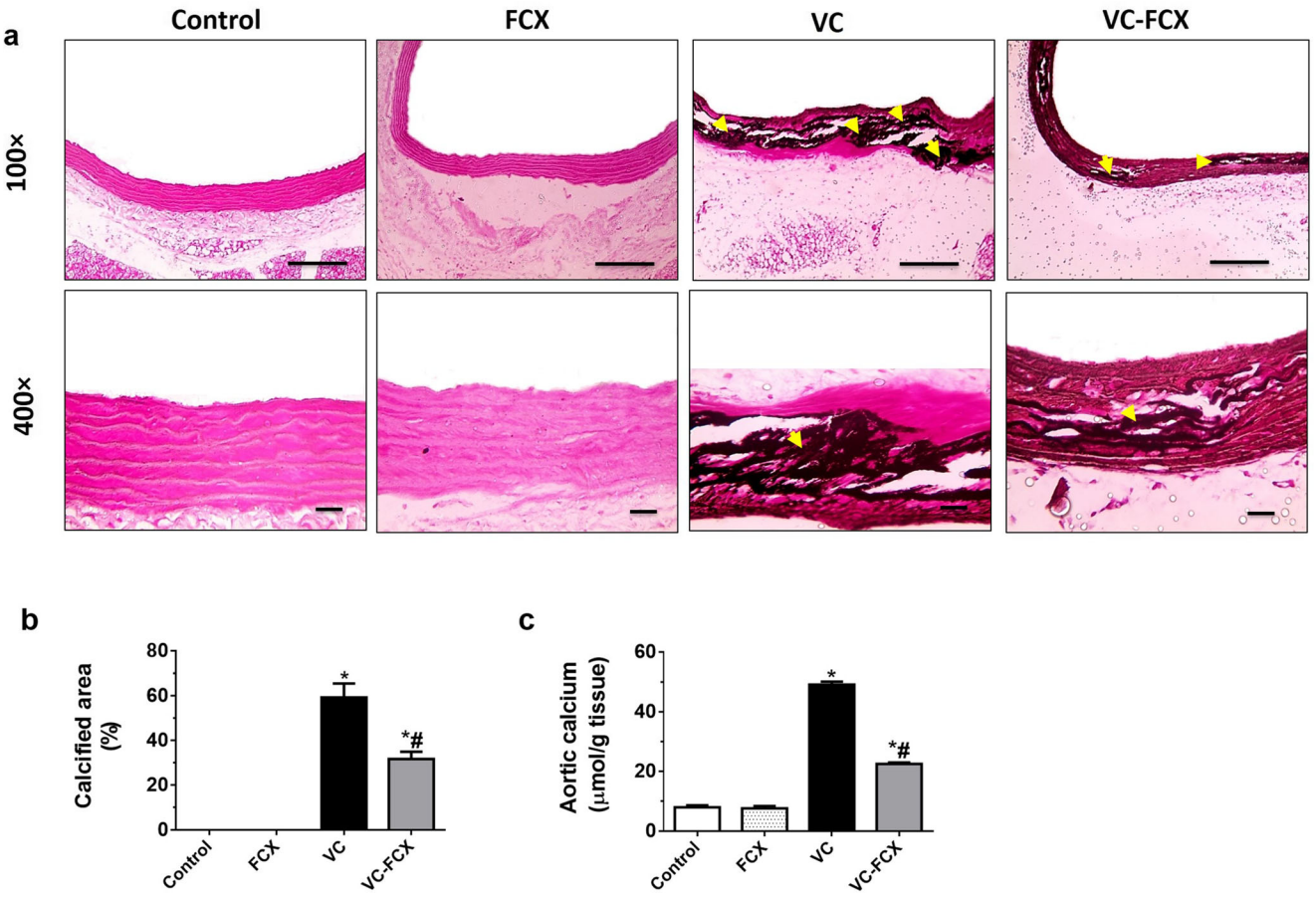

Fig. 2 Flavocoxid attenuated aortic calcium deposition in hypervitaminosis D_3 plus nicotine-administered rats. **(a)** Microimages of von Kossa staining of aortic tissues. Black areas indicate calcium deposition in the arterial wall (yellow arrowheads). Scale bars, 100 μm (for 100× magnifications) and 50 μm (for 400× magnifications) **(b)** Analysis of percentage area of aortic calcium accumulation calculated from acquired images. **(c)** Calcium content in aortic tissues assessed by o-cresolphthalein complexone method. Data are shown as means ± SEM, $n = 8$ rats per group. *, # $p < 0.05$ vs. control and VC groups, respectively. FCX, flavocoxid; VC, vascular calcification

(percentage calcified area = 31.8 ± 3.3%, $p < 0.0001$ vs. control and $p < 0.001$ vs. VC group).

Quantitative determination of aortic calcium load in VC aortas revealed a significant increase in calcium content compared to control aortas (by 517.7%, $p < 0.0001$, Fig. 2c). FCX administration to VC rats significantly ameliorated aortic calcium content (by 54.1%, $p < 0.0001$ vs. control and untreated VC groups).

Aortic Oxidative Stress

VC aortas displayed significant reductions in GSH content (Fig. 3a, by 60.5%) and SOD activity (Fig. 3b, by 56.0%) and a significant increase in MDA levels (Fig. 3c, by 185.2%) relative to control rats. FCX treatment failed to alter VC-induced decreases in aortic levels of GSH or SOD, However, it elicited a significant reduction in aortic MDA content (by 81.9%, $p < 0.0001$ vs. VC group).

Vascular Inflammatory Markers

The tunica media of aortic walls in VC rats showed moderate positive immunoreactivity against TNF-α (**Fig. 4a**). Marked immunoexpression for iNOS protein was also evident in tunica media and tunica adventitia of VC aortas (Fig. 4b). In contrast, control aortic tissues showed negative immunostaining for TNF-α and mild positive immunostaining for iNOS in tunica adventitia. Aortas from the VC-FCX group displayed reduced immunoreactivity against TNF-α and iNOS proteins. A semi-quantitative analysis of TNF-α and iNOS immunopositivity in aortic tissues is presented in Fig. 4c and d, respectively.

Moreover, aortas from VC rats displayed significant increases in aortic IL-1β levels (Fig. 4e, by 175.2%), compared with those of the control group. Treatment with FCX significantly diminished aortic IL-1β levels (by 39.8%, $p < 0.0001$ vs. VC group).

Markers of Aortic Smooth Muscle Cell Transdifferentiation

Aortas from the VC group showed significantly higher levels of Runx2 (Fig. 5a, by 33.1%) compared to those of the control group. Aortic protein levels of OPN were not significantly different between control and VC groups (Fig. 5b). FCX treatment significantly lessened Runx2 levels (by 15.5%, $p < 0.0001$) and significantly increased OPN levels (by 27.3%, $p < 0.0001$) in VC aortas compared to levels in untreated rats.

Moreover, immunohistochemical examination revealed that control aortas showed negative expression of MMP-9 (Fig. 6a) and strong brown immunostaining for the smooth muscle lineage marker α-SMA in tunica media (Fig. 6b). Conversely, aortic tissues from VC rats displayed strong positive immunoreactivity against MMP-9 in tunica media. Moreover, aortic α-SMA immunostaining was markedly reduced in the VC group.

FCX administration to VC rats substantially diminished aortic MMP-9 immunoexpression and greatly restored α-

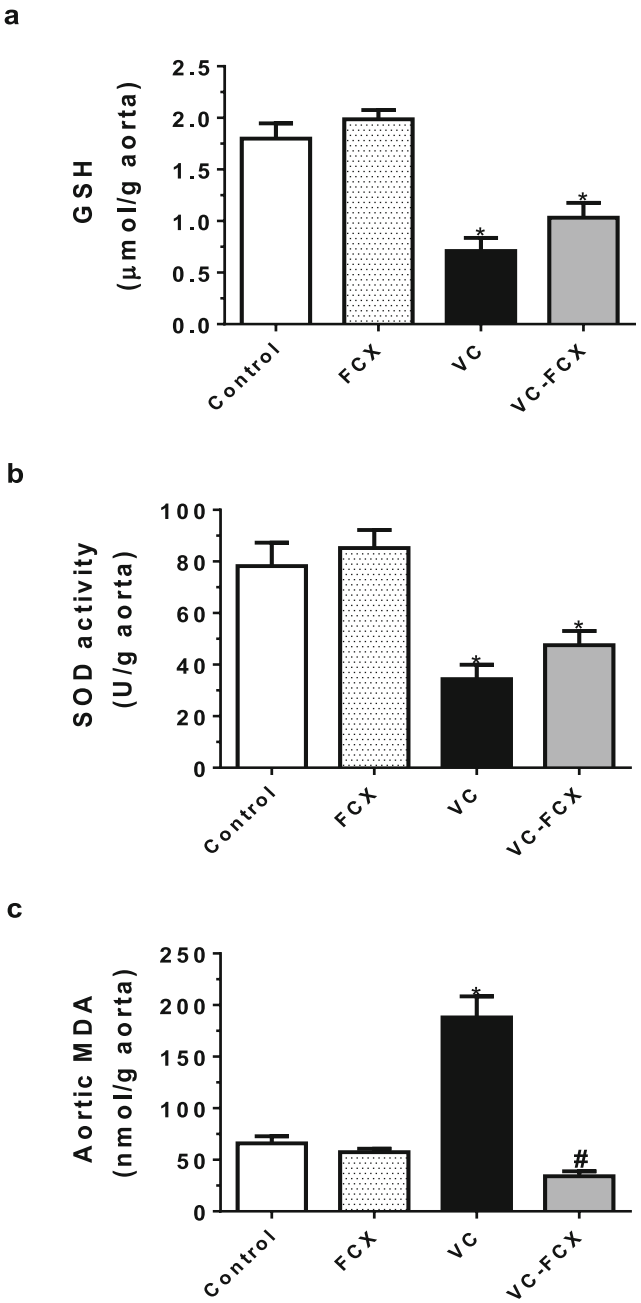

Fig. 3 Flavocoxid mitigated aortic lipid peroxidation in hypervitaminosis D_3 plus nicotine-administered rats. **(a), b)** and **(c)** Aortic tissue levels of GSH, SOD activity, and the lipid peroxidation product MDA, respectively. Data are shown as means ± SEM, $n = 8$ rats per group. $^{*,\#}p < 0.05$ vs. control and VC groups, respectively. FCX, flavocoxid; GSH, reduced glutathione; MDA, malondialdehyde; SOD, superoxide dismutase; VC, vascular calcification

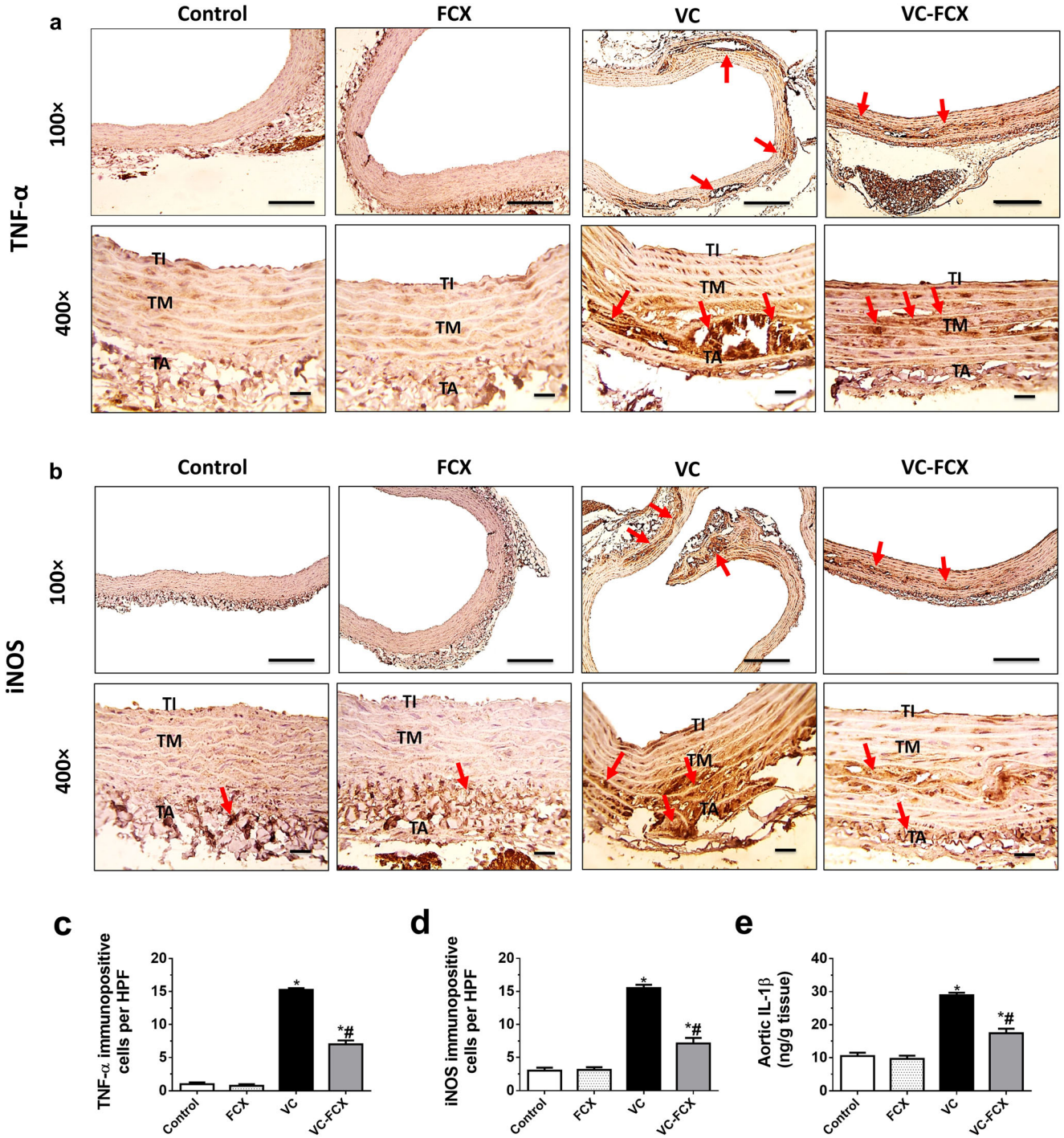

Fig. 4 Flavocoxid lessened aortic expression of TNF-α and iNOS and decreased aortic levels of IL-1β in hypervitaminosis D_3 plus nicotine-administered rats. **(a) and (b)** and **(b)** plus nicotine-administered rats. (a) and (b) Immunohistochemical aortic expression of TNF-α and iNOS, respectively. Red arrows indicate positive immunoreactivity for stained proteins. Scale bars, 100 μm (for 100× magnifications) and 50 μm (for 400× magnifications). **(c)** and **(d)** Semi-quantitative analysis of aortic TNF-α- and iNOS-immunopositive cells, respectively. **(e)** Aortic IL-1β levels. Data are shown as means ± SEM, $n = 8$ rats per group. $^{*,\#}p < 0.05$ vs. control and VC groups, respectively. FCX, flavocoxid; HPF, high power field; iNOS, inducible nitric oxide synthase; IL-1β, interleukin-1β; TNF-α, tumor necrosis factor-α; VC, vascular calcification

SMA expression in tunica media of aortic walls. A semi-quantitative analysis of MMP-9 and α-SMA immunopositivity in aortic tissues is presented in Fig. 6c and d, respectively.

Discussion

VC frequently occurs in diabetic patients and those with chronic kidney disease and may predispose patients to serious

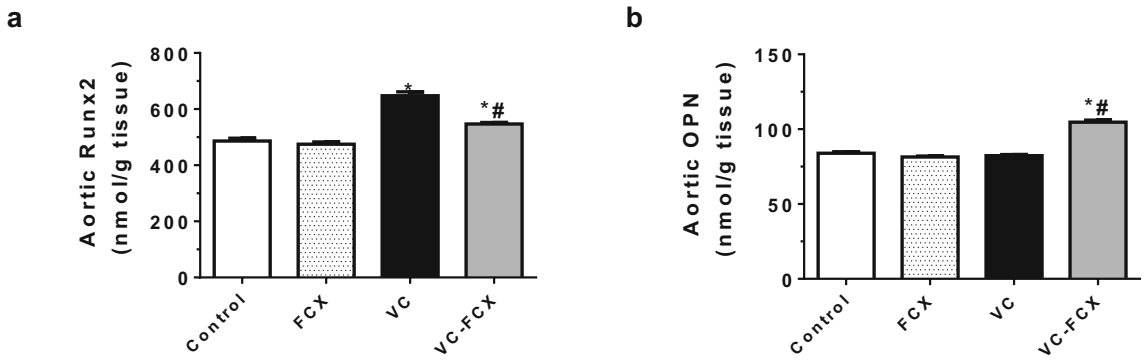

Fig. 5 Flavocoxid diminished smooth muscle cell phenotypic transition in aortas from hypervitaminosis D_3 plus nicotine-administered rats. **(a)** and **(b)** Aortic levels of the osteogenic markers Runx2 and OPN, respectively. Data are shown as means ± SEM, $n = 8$ rats per group. $^{*,\#}p < 0.05$ vs. control and VC groups, respectively. FCX, flavocoxid; OPN, osteopontin; Runx2, runt-related transcription factor 2; VC, vascular calcification

cardiovascular events [50, 51]. The VDN rat model is reported to exhibit numerous resemblances with VC occurring in diabetes, end-stage renal disease, and human arteriosclerosis [19, 20]. In the present research, FCX administration attenuated calcium deposition in aortic walls, prevented BW loss, improved hemodynamic function, restored normal cardiac rhythm, and ameliorated LV hypertrophy in hypervitaminosis D_3 plus nicotine-administered rats.

Aortic calcification in VC rats was confirmed via von Kossa staining and analysis of calcified areas in microimages of von Kossa-stained aortic sections. Moreover, VC aortas showed significantly higher calcium content, by 517.7%, than control levels. These results are in line with previous studies [52, 53]. Rats of the VC group also showed significantly lower BW than control rats, as reported previously [10, 52]. BW loss in VC rats is potentially attributed to hypervitaminosis D_3 [54, 55]. FCX treatment significantly reduced aortic calcium deposition and inhibited loss of weight in VC rats.

Moreover, VC rats showed significant elevations in SBP and DBP, marked bradycardia, and significant increases in HW/BW and LVW/BW ratios compared to control measurements. VC-induced systolic hypertension is mainly related to arterial wall stiffness brought about by increased calcium burden in vessel walls [56–58]. Cardiac alterations observed in the VC group could be caused by ventricular hypertrophy due to a prolonged increase in aortic stiffness [59–61]. FCX administration prevented rises in blood pressures, inhibited bradycardia, and reduced LV hypertrophy in VC rats, potentially via attenuating calcium deposition in aortic walls and thus impairing cardiac compensatory reflexes.

Renal function was potentially impaired in VC rats since their serum levels of creatinine and uric acid were significantly elevated compared to those of control rats. A possible explanation is that VDN elicited renal tissue calcification, promoting structural and functional damage in kidneys, as reported previously [62]. Moreover, VC rats demonstrated marked hyperphosphatemia and hypocalcemia compared to control rats. These serum ion level changes are potentially related to vitamin D_3 intoxication [63] and VDN-induced kidney damage [64]. Moreover, VC rats exhibited significantly higher serum ALP levels than control values, as reported previously [65].

FCX treatment improved kidney function and mitigated VDN-induced changes in serum levels of phosphorus, calcium, and ALP in the VC group. FCX previously attenuated the nephrotoxic effect of gentamicin in rats [29]. The ability of FCX to prevent hyperphosphatemia and reduce serum ALP activity in VC rats may play part in its capacity to alleviate aortic calcification. VSMCs cultured in hyperphosphatemic media underwent an osteogenic phenotype shift [66] and rats chronically fed a high phosphate diet suffered from aortic calcification [67]. Moreover, ALP triggers vessel calcification by reducing levels of inorganic pyrophosphate, an established inhibitor of VC [68].

Oxidative stress is a central contributor to VC pathogenesis. In this work, aortas from VC rats showed a significant increase in MDA levels and significant reductions in SOD activity and GSH levels compared to control rats. FCX treatment significantly decreased aortic levels of MDA in VC rats, while it failed to improve aortic levels of GSH and SOD activity. This paradox could be explained on the basis that lipid peroxidation is one of the pathways of arachidonic acid metabolism, which are suppressed by FCX [25]. Nevertheless, the antioxidant potential of FCX potentially contributed to its ability to attenuate aortic calcification in VC rats. It was shown that high levels of ROS induced osteogenic transdifferentiation and calcification of VSMC [12, 69, 70], possibly via enhancing the expression of the osteogenic transcription factor Runx2 [12]. Supporting this notion, high ROS levels were located with Runx2 in calcified human aortic valves, whereas the expression and activity of cellular antioxidants, including SOD and catalase, were diminished [71]. Oxidative damage may also elevate the expression of pro-inflammatory proteins [72].

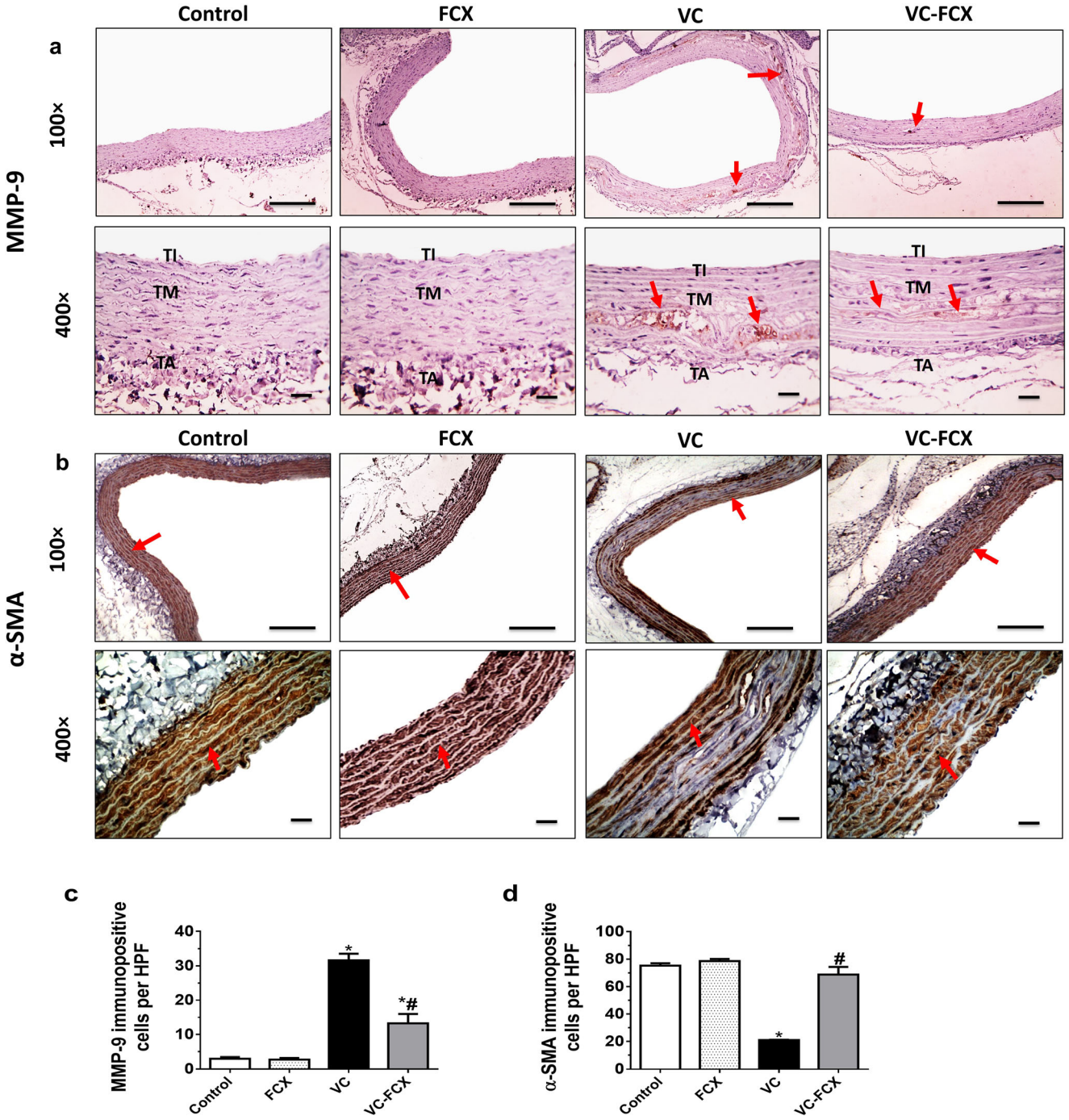

Fig. 6 Flavocoxid attenuated expression of MMP-9 and restored α-SMA expression in aortas of hypervitaminosis D3 plus nicotine-administered rats. **(a)** and **(b)** Immunohistochemical aortic expression of MMP-9 and the smooth muscle lineage marker α-SMA, respectively. Scale bars, 100 μm (for 100× magnifications) and 50 μm (for 400× magnifications). Red arrows indicate positive immunoreactivity for stained proteins. **(c)** and **(d)** Semi-quantitative analysis of aortic MMP-9- and α-SMA-immunopositive cells, respectively. Data are shown as means ± SEM, n = 8 rats per group. $^{*,\#}$ $p < 0.05$ *vs.* control and VC groups, respectively. α-SMA, smooth muscle actin; FCX, flavocoxid; HPF, high power field; MPP-9, matrix metalloproteinase-9; VC, vascular calcification

Significant increases in the aortic expression of IL-1β, TNF-α, and iNOS were evident in the VC group relative to control aortas. FCX reduced the aortic expression of IL-1β, TNF-α, and iNOS in VC rats compared to untreated ones, suggesting an anti-inflammatory effect of FCX. Previously, intragastric administration of catechin, one of the two components of FCX, inhibited the production of IL-1β and TNF-α in rats with adjuvant arthritis (Tang et al., 2007). Moreover, FCX administration reduced renal iNOS and MMP-9 expression

in mice with cadmium-induced nephrotoxicity (Micali et al., 2018).

Reducing aortic inflammation by FCX may mediate its attenuative effect against VDN-induced calcification. TNF-α was shown to induce in vitro vascular calcification via enhancing osteoblastic differentiation of vascular cells [73]. Moreover, aortic calcification in VDN-treated rats was substantially associated with macrophage infiltration and elevated expression of IL-1β and TNF-α (Gaillard et al., 2005). Furthermore, iNOS expression was upregulated in the aortas of rats with VC [16]. These inflammatory mediators were also reported to promote calcification in VSMC cultures [74]. It was previously reported that agents that reduced the expression of IL-1β [75], TNF-α [76], or iNOS [16] attenuated in vivo vessel calcification.

Furthermore, aortas from VC-FCX exhibited significantly diminished expression of Runx2 and MMP-9 and enhanced expression OPN and α-SMA compared to the untreated VC group. These effects potentially contributed to the beneficial influences of FCX on VC aortas.

VDN-induced aortic calcification was attributed to elevated expression of the bone-related gene Runx2 in the medial aortic area [77]. Overexpression of Runx2 was essential for high phosphate- and ROS-induced osteogenic differentiation of VSMCs [12, 78]. Suppression of Runx2 expression in VSMCs prevented ROS-mediated calcification [12]. Moreover, MMP-9 induces a procalcific environment via degrading elastic fibers in aortic walls and catabolizing other matrix proteins, thus facilitating the calcification process [17, 18, 79]. Blunting MMP-9 expression reduced VC [79, 80]. Reportedly, OPN inhibits vascular calcium deposition via binding to ionic calcium and hydroxyapatite [81–83]. Drugs that induced OPN expression attenuated cardiovascular calcification [52, 84]. Moreover, transdifferentiation of VSMCs into osteoblast-like cells is associated with loss of the smooth-muscle lineage marker α-SMA [85, 86].

A limitation of the present study is that the exact molecular mechanisms underlying how FCX reduced vascular Runx2 expression were not investigated. These mechanisms need to be explored in future research.

In conclusion, FCX mitigated aortic calcification and its cardiovascular consequences in VDN-treated rats via multiple mechanisms, including reducing hyperphosphatemia, oxidative stress and inflammation, diminishing aortic smooth muscle cell phenotypic transition (indicated by blunted expression of osteogenic switch gene Runx2), and increasing aortic expression of the mineralization inhibitor OPN and the smooth muscle contractile protein α-SMA.

Supplementary Information The online version contains supplementary material available at https://doi.org/10.1007/s10557-021-07227-6.

Acknowledgements The authors thank Dr. Mohamed F. Hamed (Department of Pathology, Faculty of Veterinary Medicine, Mansoura University) for his help with histopathological and immunohistochemical analyses in the present study.

Author's Contributions AEA, GSGS, and ARE designed and conducted experiments. AEA and GSGS analyzed data and wrote the manuscript. ARE, GSGS, MAN, and HAE supervised work and revised the manuscript. All authors read and approved the final manuscript.

Data Availability The datasets generated during and/or analyzed during the current study are available from the corresponding author on reasonable request.

Declarations

Ethics Approval All applicable international, national, and/or institutional guidelines for the care and use of animals were followed. This article does not contain any studies with human participants performed by any of the authors.

Consent to Participate Not applicable.

Consent for Publication Not applicable.

Conflict of Interest The authors declare no conflict of interest.

Informed Consent Not applicable.

References

1. Leem J, Lee IK. Mechanisms of vascular calcification: the pivotal role of pyruvate dehydrogenase kinase 4. Endocrinol Metab (Seoul). 2016;31(1):52–61.
2. Mackey RH, Venkitachalam L, Sutton-Tyrrell K. Calcifications, arterial stiffness and atherosclerosis. Adv Cardiol. 2007;44:234–44.
3. Fishbein MC, Fishbein GA. Arteriosclerosis: facts and fancy. Cardiovasc Pathol. 2015;24(6):335–42.
4. Ho CY, Shanahan CM. Medial arterial calcification: an overlooked player in peripheral arterial disease. Arterioscler Thromb Vasc Biol. 2016;36(8):1475–82.
5. Vattikuti R, Towler DA. Osteogenic regulation of vascular calcification: an early perspective. Am J Physiol-Endocrinol Metabol. 2004;286(5):E686–E96.
6. Shanahan CM, Crouthamel MH, Kapustin A, Giachelli CM. Arterial calcification in chronic kidney disease: key roles for calcium and phosphate. Circ Res. 2011;109(6):697–711.
7. Paloian NJ, Giachelli CM. A current understanding of vascular calcification in CKD. Am J Physiol-Renal Physiol. 2014;307(8):F891–900.
8. Mavridis G, Souliou E, Diza E, Symeonidis G, Pastore F, Vassiliou AM, et al. Inflammatory cytokines in insulin-treated patients with type 2 diabetes. Nutr Metab Cardiovasc Dis. 2008;18(7):471–6.
9. Yamada S, Taniguchi M, Tokumoto M, Toyonaga J, Fujisaki K, Suehiro T, et al. The antioxidant tempol ameliorates arterial medial calcification in uremic rats: important role of oxidative stress in the pathogenesis of vascular calcification in chronic kidney disease. J Bone Miner Res. 2012;27(2):474–85.
10. Gaillard V, Casellas D, Seguin-Devaux C, Schohn H, Dauça M, Atkinson J, et al. Pioglitazone improves aortic wall elasticity in a rat

model of elastocalcinotic arteriosclerosis. Hypertension. 2005;46(2):372–9.
11. Thompson B, Towler DA. Arterial calcification and bone physiology: role of the bone–vascular axis. Nat Rev Endocrinol. 2012;8(9):529.
12. Byon CH, Javed A, Dai Q, Kappes JC, Clemens TL, Darley-Usmar VM, et al. Oxidative stress induces vascular calcification through modulation of the osteogenic transcription factor Runx2 by AKT signaling. J Biol Chem. 2008;283(22):15319–27.
13. Massy ZA, Maziere C, Kamel S, Brazier M, Choukroun G, Tribouilloy C, et al. Impact of inflammation and oxidative stress on vascular calcifications in chronic kidney disease. Pediatr Nephrol. 2005;20(3):380–2.
14. Bessueille L, Magne D. Inflammation: a culprit for vascular calcification in atherosclerosis and diabetes. Cell Mol Life Sci. 2015;72(13):2475–89.
15. Bondm C. Inhibition of transcription factor NF-kappaB reduces matrix metalloproteinase-1, -3 and -9 production by vascular smooth muscle cells. Cardiovasc Res. 2001;50(3):556.
16. Chang X-y, Cui L, Wang X-z, Zhang L, Zhu D, Zhou X-r, et al. Quercetin attenuates vascular calcification through suppressed oxidative stress in adenine-induced chronic renal failure rats. Biomed Res Int 2017;2017:5716204.
17. Basalyga DM, Simionescu DT, Xiong W, Baxter BT, Starcher BC, Vyavahare NR. Elastin degradation and calcification in an abdominal aorta injury model: role of matrix metalloproteinases. Circulation. 2004;110(22):3480–7.
18. Pai A, Leaf EM, El-Abbadi M, Giachelli CM. Elastin degradation and vascular smooth muscle cell phenotype change precede cell loss and arterial medial calcification in a uremic mouse model of chronic kidney disease. Am J Pathol. 2011;178(2):764–73.
19. Niederhoffer N, Bobryshev YV, Lartaud-Idjouadiene I, Giummelly P, Atkinson J. Aortic calcification produced by vitamin D3 plus nicotine. J Vasc Res. 1997;34(5):386–98.
20. Gong C, Li L, Qin C, Wu W, Liu Q, Li Y, et al. The involvement of Notch1-RBP-Jk/Msx2 signaling pathway in aortic calcification of diabetic nephropathy rats. Journal of diabetes research. 2017;2017:8968523.
21. Tang F, Chen S, Wu X, Wang T, Chen J, Li J, et al. Hypercholesterolemia accelerates vascular calcification induced by excessive vitamin D via oxidative stress. Calcif Tissue Int. 2006;79(5):326–39.
22. Wallin R, Wajih N, Greenwood GT, Sane DC. Arterial calcification: a review of mechanisms, animal models, and the prospects for therapy. Med Res Rev. 2001;21(4):274–301.
23. Burnett B, Jia Q, Zhao Y, Levy R. A medicinal extract of Scutellaria baicalensis and Acacia catechu acts as a dual inhibitor of cyclooxygenase and 5-lipoxygenase to reduce inflammation. J Med Food. 2007;10(3):442–51.
24. Altavilla D, Squadrito F, Bitto A, Polito F, Burnett B, Di Stefano V, et al. Flavocoxid, a dual inhibitor of cyclooxygenase and 5-lipoxygenase, blunts pro-inflammatory phenotype activation in endotoxin-stimulated macrophages. Br J Pharmacol. 2009;157(8):1410–8.
25. Burnett BP, Bitto A, Altavilla D, Squadrito F, Levy RM, Pillai L. Flavocoxid inhibits phospholipase A2, peroxidase moieties of the cyclooxygenases (COX), and 5-lipoxygenase, modifies COX-2 gene expression, and acts as an antioxidant. Mediat Inflamm. 2011;2011:385780.
26. Messina S, Bitto A, Aguennouz M, Mazzeo A, Migliorato A, Polito F, et al. Flavocoxid counteracts muscle necrosis and improves functional properties in mdx mice: a comparison study with methylprednisolone. Exp Neurol. 2009;220(2):349–58.
27. Polito F, Bitto A, Irrera N, Squadrito F, Fazzari C, Minutoli L, et al. Flavocoxid, a dual inhibitor of cyclooxygenase-2 and 5-lipoxygenase, reduces pancreatic damage in an experimental model of acute pancreatitis. Br J Pharmacol. 2010;161(5):1002–11.
28. Bitto A, Minutoli L, David A, Irrera N, Rinaldi M, Venuti FS, et al. Flavocoxid, a dual inhibitor of COX-2 and 5-LOX of natural origin, attenuates the inflammatory response and protects mice from sepsis. Crit Care. 2012;16(1):R32.
29. El-Kashef DH, El-Kenawi AE, Suddek GM, Salem HA. Flavocoxid attenuates gentamicin-induced nephrotoxicity in rats. Naunyn Schmiedeberg's Arch Pharmacol. 2015;388(12):1305–15.
30. Abdelaziz RR, Elmahdy MK, Suddek GM. Flavocoxid attenuates airway inflammation in ovalbumin-induced mouse asthma model. Chem Biol Interact. 2018;292:15–23.
31. Micali A, Pallio G, Irrera N, Marini H, Trichilo V, Puzzolo D, et al. Flavocoxid, a natural antioxidant, protects mouse kidney from cadmium-induced toxicity. Oxidative Med Cell Longev. 2018;2018:9162946.
32. Singh DP, Chopra K. Flavocoxid, dual inhibitor of cyclooxygenase-2 and 5-lipoxygenase, exhibits neuroprotection in rat model of ischaemic stroke. Pharmacol Biochem Behav. 2014;120:33–42.
33. El-Sheakh AR, Ghoneim HA, Suddek GM, el SM A. Antioxidant and anti-inflammatory effects of flavocoxid in high-cholesterol-fed rabbits. Naunyn Schmiedeberg's Arch Pharmacol. 2015;388(12):1333–44.
34. Ding L, Jia C, Zhang Y, Wang W, Zhu W, Chen Y, et al. Baicalin relaxes vascular smooth muscle and lowers blood pressure in spontaneously hypertensive rats. Biomed Pharmacother. 2019;111:325–30.
35. Ku SK, Bae JS. Baicalin, baicalein and wogonin inhibits high glucose-induced vascular inflammation in vitro and in vivo. BMB Rep. 2015;48(9):519–24.
36. Ihm SH, Lee JO, Kim SJ, Seung KB, Schini-Kerth VB, Chang K, et al. Catechin prevents endothelial dysfunction in the prediabetic stage of OLETF rats by reducing vascular NADPH oxidase activity and expression. Atherosclerosis. 2009;206(1):47–53.
37. Koga T, Meydani M. Effect of plasma metabolites of (+)-catechin and quercetin on monocyte adhesion to human aortic endothelial cells. Am J Clin Nutr. 2001;73(5):941–8.
38. Zhang J, Chang J-R, Duan X-H, Yu Y-R, Zhang B-H. Thyroid hormone attenuates vascular calcification induced by vitamin D3 plus nicotine in rats. Calcif Tissue Int. 2015;96(1):80–7.
39. Atkinson J, Poitevin P, Chillon JM, Lartaud I, Levy B. Vascular ca overload produced by vitamin D3 plus nicotine diminishes arterial distensibility in rats. Am J Phys. 1994;266(2 Pt 2):H540–7.
40. Morgan SL, Baggott JE, Moreland L, Desmond R, Kendrach AC. The safety of flavocoxid, a medical food, in the dietary management of knee osteoarthritis. J Med Food. 2009;12(5):1143–8.
41. Burnett BP, Silva S, Mesches MH, Wilson S, Jia Q. Safety evaluation of a combination, defined extract of Scutellaria baicalensis and *Acacia catechu.* Journal of Food Biochemistry. 2007;31(6):797–825.
42. Minutoli L, Marini H, Rinaldi M, Bitto A, Irrera N, Pizzino G, et al. A dual inhibitor of cyclooxygenase and 5-lipoxygenase protects against kainic acid-induced brain injury. NeuroMolecular Med. 2015;17(2):192–201.
43. Thorin E, Henrion D, Oster L, Thorin-Trescases N, Capdeville C, Martin JA, et al. Vascular calcium overload produced by administration of vitamin D3 and nicotine in rats. Changes in tissue calcium levels, blood pressure, and pressor responses to electrical stimulation or norepinephrine in vivo. J Cardiovasc Pharmacol. 1990;16(2):257–66.
44. Wu SY, Pan CS, Geng B, Zhao J, Yu F, Pang YZ, et al. Hydrogen sulfide ameliorates vascular calcification induced by vitamin D3 plus nicotine in rats 1. Acta Pharmacol Sin. 2006;27(3):299–306.
45. Holmar J, Noels H, Bohm M, Bhargava S, Jankowski J, Orth-Alampour S. Development, establishment and validation of

in vitro and ex vivo assays of vascular calcification. Biochem Biophys Res Commun. 2020;530(2):462–70.
46. Amin FM, Abdelaziz RR, Hamed MF, Nader MA, Shehatou GSG. Dimethyl fumarate ameliorates diabetes-associated vascular complications through ROS-TXNIP-NLRP3 inflammasome pathway. Life Sci. 2020;256:117887.
47. Neumann L, Mueller M, Moos V, Heller F, Meyer TF, Loddenkemper C, et al. Mucosal inducible NO synthase-producing IgA+ plasma cells in helicobacter pylori-infected patients. J Immunol. 2016;197(5):1801–8.
48. Tsai TH, Chai HT, Sun CK, Yen CH, Leu S, Chen YL, et al. Obesity suppresses circulating level and function of endothelial progenitor cells and heart function. J Transl Med. 2012;10:137.
49. Konopelski P, Ufnal M. Electrocardiography in rats: a comparison to human. Physiol Res. 2016;65(5):717–25.
50. Moe SM, Chen NX. Pathophysiology of vascular calcification in chronic kidney disease. Circ Res. 2004;95(6):560–7.
51. Shao J-S, Cheng S-L, Sadhu J, Towler DA. Inflammation and the osteogenic regulation of vascular calcification: a review and perspective. Hypertension. 2010;55(3):579–92.
52. Cai Y, Teng X, Pan C-S, Duan X-H, Tang C-S, Qi Y-F. Adrenomedullin up-regulates osteopontin and attenuates vascular calcification via the cAMP/PKA signaling pathway. Acta Pharmacol Sin. 2010;31(10):1359.
53. G-z L, Jiang W, Zhao J, Pan C-s, Cao J, C-s T, et al. Ghrelin blunted vascular calcification in vivo and in vitro in rats. Regul Pept. 2005;129(1–3):167–76.
54. Chavhan SG, Brar RS, Banga HS, Sandhu HS, Sodhi S, Gadhave PD, et al. Clinicopathological studies on vitamin D(3) toxicity and therapeutic evaluation of Aloe vera in rats. Toxicol Int. 2011;18(1):35–43.
55. Khosravi ZS, Kafeshani M, Tavasoli P, Zadeh AH, Entezari MH. Effect of vitamin D supplementation on weight loss, glycemic indices, and lipid profile in obese and overweight women: a clinical trial study. Int J Prev Med. 2018;9:63.
56. Shi Y, Wang S, Peng H, Lv Y, Li W, Cheng S, et al. Fibroblast growth factor 21 attenuates vascular calcification by alleviating endoplasmic reticulum stress mediated apoptosis in rats. Int J Biol Sci. 2019;15(1):138–47.
57. Yang R, Teng X, Li H, Xue H-M, Guo Q, Xiao L, et al. Hydrogen sulfide improves vascular calcification in rats by inhibiting endoplasmic reticulum stress. Oxidative Med Cell Longev. 2016;2016:9095242.
58. Liu Y, Zhou YB, Zhang GG, Cai Y, Duan XH, Teng X, et al. Cortistatin attenuates vascular calcification in rats. Regul Pept. 2010;159(1–3):35–43.
59. Lartaud-Idjouadiene I, Lompré A-M, Kieffer P. Colas Trs, Atkinson J. cardiac consequences of prolonged exposure to an isolated increase in aortic stiffness. Hypertension. 1999;34(1):63–9.
60. Niederhoffer N, Lartaud-Idjouadiene I, Giummelly P, Duvivier C, Peslin R, Atkinson J. Calcification of medial elastic fibers and aortic elasticity. Hypertension. 1997;29(4):999–1006.
61. Lartaud-Idjouadiene I, Niederhoffer N, Debets J, Struyker-Boudier H, Atkinson J, Smits J. Cardiac function in a rat model of chronic aortic stiffness. Am J Phys Heart Circ Phys. 1997;272(5):H2211–H8.
62. Shi Y-C, Lu W-W, Hou Y-L, Fu K, Gan F, Cheng S-J, et al. Protection effect of exogenous fibroblast growth factor 21 on the kidney injury in vascular calcification rats. Chin Med J. 2018;131(5):532.
63. Stabley JN, Towler DA. Arterial calcification in diabetes mellitus: preclinical models and translational implications. Arterioscler Thromb Vasc Biol. 2017;37(2):205–17.
64. Terai K, Nara H, Takakura K, Mizukami K, Sanagi M, Fukushima S, et al. Vascular calcification and secondary hyperparathyroidism of severe chronic kidney disease and its relation to serum phosphate and calcium levels. Br J Pharmacol. 2009;156(8):1267–78.
65. Li Z, Huang Y, Du J, Liu A, Tang C, Qi Y, et al. Endogenous sulfur dioxide inhibits vascular calcification in association with the TGF-β/Smad signaling pathway. Int J Mol Sci. 2016;17(3):266.
66. Giachelli CM. The emerging role of phosphate in vascular calcification. Kidney Int. 2009;75(9):890–7.
67. Cozzolino M, Dusso AS, Liapis H, Finch J, Lu Y, Burke SK, et al. The effects of sevelamer hydrochloride and calcium carbonate on kidney calcification in uremic rats. J Am Soc Nephrol. 2002;13(9):2299–308.
68. Lomashvili KA, Cobbs S, Hennigar RA, Hardcastle KI, O'Neill WC. Phosphate-induced vascular calcification: role of pyrophosphate and osteopontin. J Am Soc Nephrol. 2004;15(6):1392–401.
69. Mody N, Parhami F, Sarafian TA, Demer LL. Oxidative stress modulates osteoblastic differentiation of vascular and bone cells. Free Radic Biol Med. 2001;31(4):509–19.
70. Zhao MM, Xu MJ, Cai Y, Zhao G, Guan Y, Kong W, et al. Mitochondrial reactive oxygen species promote p65 nuclear translocation mediating high-phosphate-induced vascular calcification in vitro and in vivo. Kidney Int. 2011;79(10):1071–9.
71. Miller JD, Chu Y, Brooks RM, Richenbacher WE, Peña-Silva R, Heistad DD. Dysregulation of antioxidant mechanisms contributes to increased oxidative stress in calcific aortic valvular stenosis in humans. J Am Coll Cardiol. 2008;52(10):843–50.
72. Hussain T, Tan B, Yin Y, Blachier F, Tossou MC, Rahu N. Oxidative stress and inflammation: what polyphenols can do for us? Oxidative Med Cell Longev. 2016;2016:7432797.
73. Tintut Y, Patel J, Parhami F, Demer LL. Tumor necrosis factor-alpha promotes in vitro calcification of vascular cells via the cAMP pathway. Circulation. 2000;102(21):2636–42.
74. Lencel P, Delplace S, Pilet P, Leterme D, Miellot F, Sourice S, et al. Cell-specific effects of TNF-α and IL-1β on alkaline phosphatase: implication for syndesmophyte formation and vascular calcification. Lab Investig. 2011;91(10):1434.
75. Awan Z, Denis M, Roubtsova A, Essalmani R, Marcinkiewicz J, Awan A, et al. Reducing vascular calcification by anti-IL-1β monoclonal antibody in a mouse model of familial hypercholesterolemia. Angiology. 2016;67(2):157–67.
76. Lin C-P, Huang P-H, Lai CF, Chen J-W, Lin S-J, Chen J-S. Simvastatin attenuates oxidative stress, NF-κB activation, and artery calcification in LDLR−/−mice fed with high fat diet via down-regulation of tumor necrosis factor-α and TNF receptor 1. PLoS One. 2015;10(12):e0143686.
77. Han MS, Che X, Cho GH, Park HR, Lim KE, Park NR, et al. Functional cooperation between vitamin D receptor and Runx2 in vitamin D-induced vascular calcification. PLoS One. 2013;8(12):e83584.
78. Yoshida T, Yamashita M, Hayashi M. Kruppel-like factor 4 contributes to high phosphate-induced phenotypic switching of vascular smooth muscle cells into osteogenic cells. J Biol Chem. 2012;287(31):25706–14.
79. Hecht E, Freise C. Websky Kv, Nasser H, Kretzschmar N, Stawowy P, et al. the matrix metalloproteinases 2 and 9 initiate uraemic vascular calcifications. Nephrology Dialysis Transplantation. 2015;31(5):789–97.
80. Qin X, Corriere MA, Matrisian LM, Guzman RJ. Matrix metalloproteinase inhibition attenuates aortic calcification. Arterioscler Thromb Vasc Biol. 2006;26(7):1510–6.
81. Bäck M, Aranyi T, Cancela ML, Carracedo M, Conceição N, Leftheriotis G, et al. Endogenous calcification inhibitors in the prevention of vascular calcification: a consensus statement from the COST action EuroSoftCalcNet. Frontiers in cardiovascular medicine. 2018;5:196.

82. Scatena M, Liaw L, Giachelli CM. Osteopontin: a multifunctional molecule regulating chronic inflammation and vascular disease. Arterioscler Thromb Vasc Biol. 2007;27(11):2302–9.
83. Paloian NJ, Leaf EM, Giachelli CM. Osteopontin protects against high phosphate-induced nephrocalcinosis and vascular calcification. Kidney Int. 2016;89(5):1027–36.
84. Wang F, Jiang T, Tang C, Su Z, Zhang N, Li G. Ghrelin reduces rat myocardial calcification induced by nicotine and vitamin D3 in vivo. Int J Mol Med. 2011;28(4):513–9.
85. Zhang X, Li R, Qin X, Wang L, Xiao J, Song Y, et al. Sp1 plays an important role in vascular calcification both in vivo and in vitro. J Am Heart Assoc. 2018;7(6):e007555.
86. Steitz SA, Speer MY, Curinga G, Yang HY, Haynes P, Aebersold R, et al. Smooth muscle cell phenotypic transition associated with calcification: upregulation of Cbfa1 and downregulation of smooth muscle lineage markers. Circ Res. 2001;89(12):1147–54.